DALTON
FULL PAPER

Structural studies of complexes of vanadium(III) and titanium(IV) with *N*,*N*-dimethylaminomethylferrocenyl

Peter B. Hitchcock,[a] David L. Hughes,[b] G. Jeffery Leigh,[a] J. Roger Sanders[b] and Jaísa S. de Souza[c]

[a] *School of Chemistry, Physics and Environmental Science, University of Sussex, Brighton, UK BN1 9QJ*
[b] *Nitrogen Fixation Laboratory, John Innes Centre, Norwich Research Park, Colney, Norwich, UK NR4 7UH*
[c] *Departamento de Química, Universidade do Paraná, Centro Politécnico, Jardim das Americas, 81531-990 Curitiba-PR, Brasil*

Received 9th November 1998, Accepted 16th February 1999

Vanadium(III) and titanium(IV) complexes containing 12–16 valence-shell electrons have been synthesised by treatment of cyclopentadienylmetal halides with the lithium salt of *N*,*N*-dimethylaminomethylferrocene, Li(FcN). The structurally characterized products were $[(\eta^5\text{-}C_5H_5)_2Ti(\eta^1\text{-}FcN)Cl]$ **1**, $[(\eta^5\text{-}C_5H_5)Ti(FcN)_xCl_{3-x}]$ ($x = 1$, complex **2**; $x = 2$, complex **3**; and $x = 3$, complex **4**) and $[V(FcN)_2Cl]$ **6**. They contain FcN bound either monodentate, through the aromatic 2-carbon atom, or bidentate, through that carbon and the amine nitrogen. Despite employing a variety of spectroscopic techniques, we were unable to distinguish the mode of binding in any way other than a crystal structure analysis. Compound **4** changes spontaneously at room temperature into the structurally characterised $[(\eta^5\text{-}C_5H_5)Ti(FcN)(FcN')]$ **5**. The ligand FcN′ arises by metallation of one methyl group of one FcN in **4** with elimination of H(FcN). This kind of metallation has not been recognised hitherto in titanium or vanadium FcN chemistry, and it may explain why yields of required products are sometimes very low. The synthetic and structural versatility of the ligand FcN have been clearly demonstrated.

We have recently been interested in creating vanadium compounds that would fix nitrogen, in which there are additional redox-active metal atoms not involved in dinitrogen binding. These might contribute electrons to any protonation reaction of dinitrogen, and thus affect the mechanism of protonation and the yields of reduced products. We decided finally that the incorporation of *N*,*N*-dimethylaminomethylferrocenyl (FcN) into dinitrogen-binding compounds might provoke the kind of chemistry that we desired.

We initially had two target systems in mind. One was analogous to the bridging dinitrogen system originally discovered by Gambarotta *et al.*,[1] namely $[\{V(C_6H_4CH_2NMe_2\text{-}2)_2(C_5H_5N)\}_2(\mu\text{-}N_2)]$, in which we hoped to replace the phenylene moiety by ferrocenyl. It is known[2] that treatment of the binuclear V^{II}–phenylene compound with acid generates ammonia, and our preliminary work showed that a mixture of $[VCl_2(tmen)_2]$ (tmen = *N*,*N*,*N*′,*N*′-tetramethylethane-1,2-diamine) and $Li[Fe(C_5H_5)(C_5H_3CH_2NMe_2)]$, Li(FcN), did indeed pick up dinitrogen.[3] The other was complexes of the type $[\{Ti(\pi\text{-}C_5H_5)_2R\}_2(\mu\text{-}N_2)]$[4] (R = benzyl or aryl) in which we hoped to replace the R group by a ferrocenyl residue. These titanium complexes can be reduced to give ammonia.[5]

There have been many attempts to use *N*,*N*-dimethylaminomethylferrocenyl as a ligand to transition metals. However, only rarely have crystalline complexes been isolated and general structural data are lacking. There are no spectral criteria to indicate whether the ferrocenyl residue is monodentate or bidentate in any given compound. Consequently it was thought worthwhile to carry out a general study of this ligand to see whether we could establish sound criteria for its mode of attachment to metals.

The use of the monolithium salt of *N*,*N*-dimethylaminomethylferrocene, Li(FcN), together with transition metal halides, as starting material for the synthesis of organobimetallic complexes dates back to the 1970s, when the first mercury–[6] and palladium–FcN[7] derivatives were described. Since then, an extensive range of compounds containing this ligand has been synthesised and characterised by IR, UV, ^1H and ^{13}C NMR spectroscopies, elemental analysis, determination of magnetic moments and thermal stabilities. In contrast, few of those organobimetallic derivatives have been analysed by X-ray crystallography.

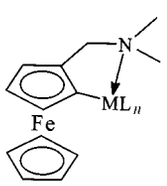

Fig. 1 FcN as a bidentate ligand.

Complexes containing FcN have been reported for several metals.[12,16–20] This ligand is often assumed to be bidentate, with the 1-carbon atom from the substituted Cp ring and the amine nitrogen acting as donors to a transition metal ion (Fig. 1). This has been demonstrated by X-ray diffraction analysis of the platinum complexes $[\{Pt(C_5H_3CH_2NMe_2)X(dmso)\}_2Fe]$[8,9] (X = Cl or Br) and of the bis(2,2-dimethylaminomethyl) derivatives of (1,1-dimercurio)ferrocenophane,[10,11] but it remained as an assumption for most of the other bimetallic products described to date. Additionally, the crystal structure analysis of complexes such as $[Cp_2M(FcN)_2]$ ($M = Ti^{IV}$ or Zr^{IV}),[12] and $[\{M(FcN)\}_4]$ ($M = Ag^+$ or Cu^+)[13,14] revealed monodentate FcN, bound to the metal ions exclusively through carbon. Another possibility has also been demonstrated by the single-crystal X-ray diffraction analysis of $[\{Cu(HFcN)X\}_4]$ (X = Cl or Br),

Table 1 ^{1}H NMR data for the starting materials and for compounds **1**–**4** and **6** in C_6D_6 (in ppm, room temperature)

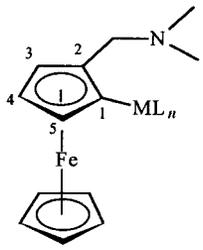

Compound	NCH_3	NCH_2	CpFe	H^3, H^4, H^5	CpTi
H(FcN)	2.11 (s, 6H)	3.19 (s, 2H)	3.96 (s, 5H)	3.94 (t, 2H) 4.08 (t, 2H)	—
$[Cp_2TiCl_2]$	—	—	—	—	5.91 (s)
$[CpTiCl_3]$	—	—	—	—	5.99 (s)
$[Cp_2Ti(FcN)Cl$	2.09 (s, 6H)	2.47 (d, 1H, J = 12.5)	4.17 (s, 5H)	3.67 (s, br, 1H)	6.00 (s, 5H)
1		3.55 (d, 1H, J = 12.5)		4.06 (t, 1H) 4.10 (m, 1H)	6.28 (s, 5H)
$[CpTi(FcN)Cl_2]$	2.14 (s, 6H)	2.41 (d, 1H, J = 12.6)	4.42 (s, 5H)	3.89 (m, 1H)	6.33 (s, 5H)
2		3.48 (d, 1H, J = 12.6)		3.93 (m, 1H) 3.98 (t, 1H)	
$[CpTi(FcN)_2Cl]$	2.10 (s, 12H)	2.61 (d, 2H, J = 12.3)	4.17 (s, 10H)	3.97 (m, 2H)	6.70 (s, 5H)
3		3.78 (d, 2H, J = 12.3)		4.08 (t, 2H) 4.86 (m, 2H)	
$[CpTi(FcN)_3]$	2.11 (s, 6H)	2.66 (d, 1H, J = 12.3)	3.84 (s)[a]	3.97 (m)[a]	7.30 (s, 5H)
4		2.74 (d, 1H, J = 12.3)		4.00 (m)[a]	
	2.18 (s, 6H)	2.77 (d, 1H, J = 12.0)[b]	3.91 (s, 5H)	4.10 (t)[c] 4.14 (t)[c]	
	2.39 (s, 6H)	3.65 (d, 1H, J = 12.2)[b]	4.17 (s, 5H)	4.29 (t, 1H) 6.11 (s, br, 1H) 6.79 (s, br, 1H)	
$[V(FcN)_2Cl]$	2.24 (s)	3.08 (d, J = 13.0)	3.98 (s)	4.10 (s, br)	
6		3.85 (d, J = 12.8)		4.23 (s, br) 4.98 (s, br)	

[a] Intensity corresponding to a total of 8H between δ 3.8–4.0. [b] Doublets hidden in the H^3, H^4, H^5 region, but presence confirmed by ^{13}C, ^{1}H-HETCOR. [c] Integration made difficult by the complexity of the spectrum in this region.

Table 2 ^{13}C-{^{1}H} NMR chemical shifts for Li(FcN) and compounds **1**–**4** (in ppm, room temperature)

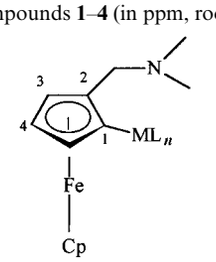

Compound	Solvent	C–M	C^2	C^3	C^4	C^5	CpFe	NCH_2	NCH_3	CpTi
Li(FcN)	thf-d_8	95.5	84.9	70.7	68.3	81.1	69.0	59.9	45.0	—
$[Cp_2Ti(FcN)Cl]$ **1**	C_6D_6	136.8	88.4	73.3	67.7	78.3	70.2	61.2	45.5	116.7, 117.2
$[CpTi(FcN)Cl_2]$ **2**	C_6D_6	166.5	88.8	70.7	69.9	75.8	73.1	61.6	46.2, 46.3	119.4
$[CpTi(FcN)_2Cl]$ **3**	C_6D_6	151.7	89.2	73.5	68.4	78.4	71.2	61.6	45.3	116.8
$[CpTi(FcN)_3]$ **4**	C_6D_6	136.2	88.4	72.0	67.7	79.6	69.5	61.6	45.2	
		143.8	89.8	75.0	68.1	81.2	69.8	62.2	45.3	115.3
		145.5	92.1	75.2	68.8	83.9	70.3	62.5	46.0	

where neutral HFcN is monodentate, connected this time to each Cu^+ ion exclusively through the amine nitrogen atom.[15]

For Group 5 metals, $[Cp_2V^{III}(FcN)]$[16,17] and $V^{IV}O(FcN)_2$·Li(MeCOCHCOMe)[18] have been described but not structurally characterised. For Nb and Ta, only the oxidation state v has been explored.[19] More recently,[20] the compounds $[VCl_{3-n}(FcN)_n]$ (n = 1, 2, or 3), $[Cp_2V^{III}(FcN)]$, $[VOCl(FcN)_2]$, $[V^{IV}O(FcN)(MeCOCHCOMe)]$ and $[Ti(FcN)_3]$ have been described in some detail, though without any structural determinations.

This current paper describes the synthesis and unequivocal characterisation of (FcN) complexes of vanadium(III) and titanium(IV). Some of these results have been published in preliminary form.[21]

Results and discussion

Complexes of titanium(IV)

The reaction of dichlorobis(cyclopentadienyl)titanium(IV) with one molar equivalent of Li(FcN) in diethyl ether at room temperature afforded the deep green diamagnetic solid $[(\eta^5\text{-}C_5H_5)_2Ti(\eta^1\text{-}FcN)Cl]$ **1** in 60% yield. It is soluble in non-polar solvents and is air-sensitive although the dark green crystals are less sensitive than its solutions.

The principal ions detected in the mass spectra (EI) of **1** (and of further compounds **2**–**6**) are presented in the Experimental section. The resonances assigned to the cyclopentadienyls bound to titanium in **1** are split in both the ^{1}H and ^{13}C NMR spectra (Tables 1 and 2). Similar splittings were not reported for

Table 3 Selected molecular dimensions in complex **1**. Bond lengths are in Ångstroms, angles in degrees. E.s.d.s are in parentheses

(a) About the metal atoms

Range of M–C lengths		Mean M–C	Distance to ring centroid[a]	
Fe–C(11–15)	2.029(6)–2.093(4)	2.055(12)	Fe–C(1m)	1.652(5)
Fe–C(21–25)	2.043(9)–2.075(11)	2.062(6)	Fe–C(2m)	1.639(10)
Fe–C(21x–25x)	1.99(2)–2.05(2)	2.025(9)	Fe–C(2xm)	1.678(16)
Ti–C(31–35)	2.386(17)–2.426(13)	2.411(7)	Ti–C(3m)	2.095(15)
Ti–C(31x–35x)	2.33(2)–2.46(2)	2.390(22)	Ti–C(3xm)	2.073(16)
Ti–C(41–45)	2.345(8)–2.388(7)	2.370(8)	Ti–C(4m)	2.051(8)
Ti–Cl	2.346(2)	Ti–C(14)	2.186(4)	
C(1m)–Fe–C(2m)	175.7(4)	C(3m)–Ti–C(4m)	132.6(5)	
C(1m)–Fe–C(2xm)	173.4(6)	C(3xm)–Ti–C(4m)	130.6(5)	
C(3m)–Ti–Cl	107.2(5)	C(3m)–Ti–C(14)	100.5(4)	
C(3xm)–Ti–Cl	105.8(5)	C(3xm)–Ti–C(14)	104.5(5)	
C(4m)–Ti–Cl	107.0(3)	C(4m)–Ti–C(14)	108.6(3)	
Cl–Ti–C(14)	94.3(1)	C(13)–C(14)–Ti	137.2(3)	
C(15)–C(14)–Ti	117.1(3)	Ti–C(14)–C(1m)	166.5(4)	

(b) In the ferrocenyl side chain

C(13)–C(131)	1.474(7)	N(132)–C(133)	1.471(10)
C(131)–N(132)	1.468(7)	N(132)–C(134)	1.410(9)
C(12)–C(13)–C(131)	121.7(5)	C(131)–N(132)–C(133)	110.2(6)
C(14)–C(13)–C(131)	129.8(5)	C(131)–N(132)–C(134)	110.7(6)
C(13)–C(131)–N(132)	113.7(5)	C(133)–N(132)–C(134)	108.0(8)

(c) Torsion angles

C(12)–C(13)–C(131)–N(132)	103.5(6)
C(14)–C(13)–C(131)–N(132)	−72.0(7)
C(11)–C(1m)–C(2m)–C(24)	3.3(8)
C(11)–C(1m)–C(2xm)–C(21x)	34.1(12)
C(31)–C(3m)–C(4m)–C(42)	−13.4(12)
C(31x)–C(3xm)–C(4m)–C(44)	−32.9(14)

[a] The suffix 'm' denotes the centroids of a Cp ring. The suffix 'x' indicates the second orientation of a disordered Cp ring.

the complex $[Cp_2Ti(FcN)_2]$.[22] The magnetic non-equivalence of the titanium Cp protons is a consequence of the presence of the single asymmetrical FcN with planar chirality in the coordination sphere of the titanium[23–25] and is not evidence for monodentate or bidentate binding.

The methylene protons of the FcN moiety of **1** are also magnetically non-equivalent. This phenomenon has been observed in the ^{1}H NMR spectra of complexes containing both monodentate and bidentate 1,2-disubstituted ferrocenyl ligands.[26–29] It is also a consequence of the asymmetry of the disubstituted Cp ring. The diasteriotopic methylene protons give rise to two AB doublets with a coupling constant of 10–14 Hz for a large range of complexes.[26] In the case of **1**, the doublets are observed at δ 2.47 (J = 12.5 Hz) and δ 3.55 (J = 12.5 Hz).

The crystal and molecular structures of **1** have been reported in a preliminary communication.[21] Selected bond dimensions are listed in Table 3. The discrete monomeric molecules are separated by normal van der Waals distances. The titanium (Fig. 2) exhibits a distorted tetrahedral coordination and binds a monodentate FcN. The average C–C bond lengths in the titanocene and ferrocene cyclopentadienyl rings are 1.392(17) Å and 1.411(15) Å, respectively. The average Fe–C(Cp) distance is 2.054(96) Å and Ti–C(Cp) 2.380(10) Å, both very similar to those in ferrocene itself[30] and in the starting material $[Cp_2TiCl_2]$.[31] However, the range of Fe–C distances is rather wider in the ring C(11–15) than in the other rings, which reflects the presence of the substituent group on C(13) and the bridging to Ti by C(14).

There are two possible orientations for one of the rings of the FcN ligand in compound **1**. The planar rings C(11)–C(15) and C(21)–C(25) are nearly eclipsed (mean torsion angle *ca.* 3°), while the cyclopentadienyl rings C(11)–C(15) and C(21x)–C(25x) show a deviation of *ca.* 2.5° from the staggered arrangement. The torsion angles were calculated as, for instance, C(11)–C(1m)–C(2m)–C(24), where C(1m) and C(2m)

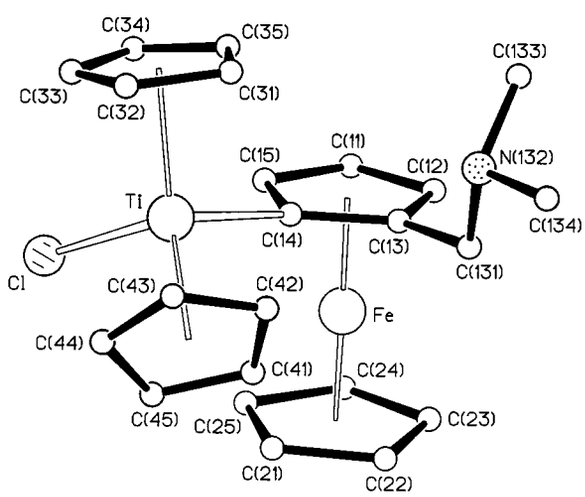

Fig. 2 Representation of the molecular structure of complex **1** (with the atom labelling scheme), showing monodentate coordination of $(FcN)^-$. The diagram was drawn with the use of the ORTEP package.[60]

are the centroids of the Cp rings C(11)–C(15) and C(21)–C(25) respectively. In the titanocene fragment, where one of the Cp rings is disordered in two orientations, there is a perfectly staggered conformation for the C(31x)–C(35x) and C(41)–C(45) rings and a small deviation of *ca.* 14.5° from the eclipsed arrangement of the C(31)–C(35) and C(41)–C(45) rings.

The Ti–C σ-bond length in **1** is 2.186(4) Å, which is essentially the same as that found in $[Cp_2Ti(Fc)_2]$[32] (Fc = ferrocenyl), 2.192(9) Å, and significantly shorter than the corresponding value of $[Cp_2Ti(FcN)_2]$, 2.235(4) Å.[12] The atom N(132) makes only normal van der Waal's contacts with the atoms of the titanocene moiety, which contrast with repulsions proposed in $[Cp_2M(FcN)_2]$ (M = Ti or Zr).[12]

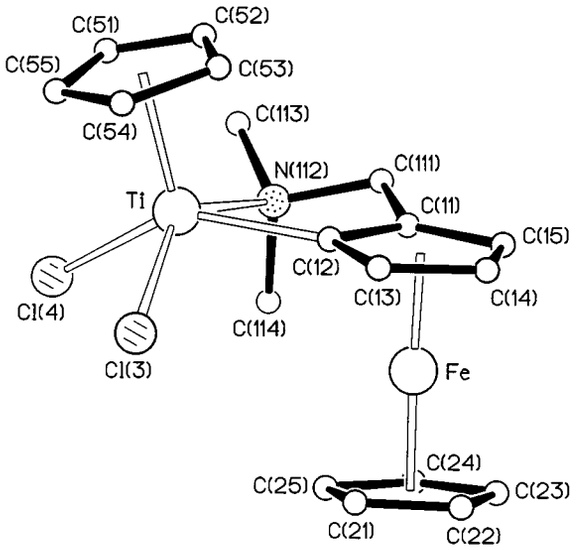

Fig. 3 Representation of the molecular structure of complex **2**, showing bidentate coordination of FcN.

The angle Cp–Ti–Cp is insensitive to other substituents, since it varies only from 129.9° to 131.6° in a range of compounds analogous to **1**.[12,31–33] The Ti–Cl bond length, 2.346(2) Å, is close to the average Ti–Cl bond distance found in $[Cp_2TiCl_2]$[31] (2.364 Å) and the angle (C14)–Ti–Cl [94.3(1)°], is much closer to the Cl–Ti–Cl angle of $[Cp_2TiCl_2]$[31] (94.53°) than to the C(6)–Ti–C(6A) angle of $[Cp_2Ti(FcN)_2]$[12] (100.7°). This suggests that the exchange of only one chloride ion in the starting material for FcN^- does not change substantially the molecular geometry. Major differences seem to arise only when the second chlorine atom is substituted.[12]

The most interesting structural feature is the lack of a chelating interaction between N(132) in the ferrocenyl side chain and the titanium atom (see Fig. 1 and 2). There are certainly vacant orbitals on the titanium that would allow bonding to occur.[34] However, MO studies imply barriers to rotation around the M–L bond in molecules $[Cp_2ML_n]$[34] and these must also be significant here. This ligand is also monodentate in $[Cp_2Ti(FcN)_2]$, $[Cp_2Zr(FcN)_2]$,[12] $[Cu_4(\mu\text{-}FcN)_4]$,[14] $[Ag_4(\mu\text{-}FcN)_4]$[13] and $[\{[1\text{-}HgCl\text{-}2\text{-}(Me_2NCH_2)C_5H_3]Fe(C_5H_5)\}_2]$,[35] although the last has a dimeric structure in the crystal due to Hg···N intermolecular interactions.

The results described above and those of Thiele and coworkers[12] show that the replacement of halides X^- in $[Cp_2TiX_2]$ by $(FcN)^-$ gives only products with monodentate FcN. Nevertheless, we still had no spectral criteria for the denticity of the FcN, and we therefore extended our studies to systems in which chelating FcN might be expected.

The reaction of $[CpTiCl_3]$[36] with one molar equivalent of Li(FcN) in diethyl ether at room temperature yielded $[CpTiCl_2(FcN)]$ **2**, the first Ti compound containing bidentate FcN characterised by X-ray crystal structure analysis.[21] It is soluble in thf, Et_2O and aromatic hydrocarbons, but only slightly soluble in hexane. When recrystallised from diethyl ether–hexane mixtures at −20 °C, the product gave deep blue, thin diamond-shaped plates suitable for X-ray analysis (Fig. 3).

Selected NMR data are listed in Tables 1 and 2. The pair of doublets in the ^1H NMR spectrum assigned to the CH_2N protons is again noteworthy. The magnetic non-equivalence is explained by the rigidity of the chelate Ti–N(112)–C(111)–C(11)–C(12) ring, which keeps both the methylene protons and the methyl groups in constrained positions (Fig. 3). This also explains the presence of two very close signals for the $N(CH_3)_2$ unit in the $^{13}C\text{-}\{^1H\}$ NMR spectrum of **2** (Table 2).

There is a shift to lower frequencies of the resonances assigned to C(1) (C bound to Ti) and to $(C_5H_5)Fe$ in the $^{13}C\text{-}\{^1H\}$ NMR spectra of the series $[CpTi(FcN)_xCl_{3-x}]$ (x = 1–3; complexes **2**–**4**) as the chlorides are replaced. This can be rationalised by the increased shielding of these carbon nuclei by the electronic density on the metal orbitals. However, the opposite sequence is revealed for C(2), C(3) and C(5) resonances. The reason is not evident. A number of studies[27] of monosubstituted ferrocenes have shown that, relative to ferrocene resonances, a single substituent may either shield or deshield positions 2 and 5 *and* shield or deshield positions 3 and 4, in any combination.

Principal molecular dimensions of $[CpTi\{(C_5H_3CH_2NMe_2)FeCp\}Cl_2]$ **2** are summarised in Table 4. The coordination around the titanium atom in **2** is square-pyramidal, with the Cp ligand in the apical position. The angle (C(12)–Ti–N(112) is 74.2(2)°, Cl(3)–Ti–Cl(4) is 89.4(1)° and the average angle L–Ti–C(5m), *i.e.*, the angle subtended by the donor atoms (C, N, Cl) and the centroid of the Cp ring, is 110.2°. These values compare well with those reported for the other square-pyramidal molecules $[(\eta^6\text{-hmb})Ti^{II}(Cl_2AlCl_2)_2]$[33] (hmb = hexamethylbenzene) and $[(\eta^5\text{-Cp})Ti^{III}(dmp)_2]$[37] [dmp = 2-(*N*,*N*-dimethylaminomethyl)phenyl]. The distance Ti–C(5m), 2.037(12) Å, is typical of a $CpTi^{IV}$ complex[33] and is rather shorter than that in **1**, which is affected by the steric effects of the two Cp rings.

The FcN ligand is bidentate, whereas in **1** it is monodentate. The comparable bond lengths in **1** and **2** are very similar except that the N–Me bonds in **2** are slightly longer than in **1**, probably a result of the chelation. The average Ti–C(Cp) bond in **2** [2.345(3) Å] and the Ti–(Cp centroid) distance (2.037 Å) are both shorter than in **1** [2.387(10) Å and 2.073 Å, respectively], explained by the presence of two sterically demanding Cp rings in the latter. The Ti–N(112) and the N(112)–Ti–C(12) dimensions are similar to those in $[Cp_2Ti(C_6H_4CH_2NMe_2)]$[39] which is a dimethylbenzylamine derivative of Ti^{III} with C and N atoms coordinated to titanium as part of a chelate ring. The chelate ring in **2** has an envelope conformation with N(112) displaced 0.48(1) Å out of the plane of the other four atoms.

Complex **2** is planar chiral due to the structural asymmetry of the five-membered chelate ring fused to the ferrocenyl moiety.[23,25] Because the FcN ligand itself does not contain any element of *central* chirality, cyclometallation should produce both the *R*- and *S*-isomers in equal proportions. Both isomers are observed in the centrosymmetric $P2_1/c$ unit cell; Fig. 3 shows a molecule with the *R*-configuration, assigned according to Marquarding *et al.*[25]

The reaction of $[CpTiCl_3]$ with two or three molar equivalents of Li(FcN) in diethyl ether proceeds easily at room temperature for the synthesis of $[CpTi(FcN)_2Cl]$ **3**, or in the range 0–20 °C for the synthesis of $[CpTi(FcN)_3]$ **4**. Both procedures are perfectly reproducible. The substitution of the halide ions in the Ti^{IV}-starting material seems to be stepwise, as suggested by the gradual colour changes observed. Both products are moderately air-sensitive and **4** is temperature-sensitive.

Both complexes can be reproducibly crystallised from saturated hexane solutions at −20 °C. This is a very slow process, taking from two weeks to two months to produce crystals of a reasonable size. Compound **3** gives thin deep blue needles which change quickly to reddish after isolation, while **4** produces very thin purple prisms. None of the crystals we obtained were suitable for X-ray structure determination.

Both ^1H and $^{13}C\text{-}\{^1H\}$ NMR spectra of **3** (Tables 1 and 2) clearly suggest that the FcN units are magnetically equivalent, as each distinct proton or carbon nucleus produces only one resonance. The integration of the peak areas in the ^1H NMR spectrum confirmed the 2:1 proportion of the $(C_5H_5)Fe$ to $(C_5H_5)Ti$ moieties. The methylene protons are again magnetically non-equivalent but *N*-methyl resonances are not split in either the ^1H or the $^{13}C\text{-}\{^1H\}$ NMR spectra. This may indicate the presence of monodentate FcN, but requires confirmation. The inversion of the order of chemical shifts for carbon and proton signals (C3 > C4, while H4 > H3), confirmed by

Table 4 Selected molecular dimensions in complex **2**. Bond lengths are in Ångstroms, angles in degrees. E.s.d.s are in parentheses

(a) About the metal atoms

Range of M–C lengths		Mean M–C	Distance to ring centroid[a]	
Fe–C(11–15)	2.027(8)–2.073(7)	2.050(10)	Fe–C(1m)	1.652(8)
Fe–C(21–25)	2.035(8)–2.045(8)	2.039(2)	Fe–C(2m)	1.655(9)
Ti–C(51–55)	2.337(9)–2.353(10)	2.345(3)	Ti–C(5m)	2.037(12)
Ti–Cl(3)	2.324(2)	T–C(12)		2.107(7)
Ti–Cl(4)	2.317(2)	Ti–N(112)		2.446(6)
C(1m)–Fe–C(2m)	174.5(4)			
C(12)–Ti–N(112)	74.2(2)	N(112)–Ti–Cl(4)		82.6(2)
C(12)–Ti–Cl(3)	86.0(1)	N(112)–Ti–C(5m)		110.1(4)
C(12)–Ti–Cl(4)	139.2(2)	Cl(3)–Ti–Cl(4)		89.4(1)
C(12)–Ti–C(5m)	107.1(4)	Cl(3)–Ti–C(5m)		111.4(4)
N(112)–Ti–Cl(3)	137.7(2)	Cl(4)–Ti–C(5m)		112.3(4)
C(11)–C(12)–Ti	119.6(5)	Ti–C(12)–C(1m)		172.3(6)
C(13)–C(12)–Ti	133.9(6)	C(111)–N(112)–Ti		108.3(4)

(b) In the ferrocenyl side chain

C(11)–C(111)	1.471(10)	N(112)–C(113)	1.513(10)
C(111)–N(112)	1.485(9)	N(112)–C(114)	1.496(9)
C(12)–C(11)–C(111)	119.1(6)	C(111)–N(112)–C(113)	108.8(6)
C(15)–C(11)–C(111)	130.8(7)	C(111)–N(112)–C(114)	108.0(6)
C(11)–C(111)–N(112)	110.7(6)	C(113)–N(112)–C(114)	106.1(7)

(c) Torsion angles

Ti–C(12)–C(11)–C(111)	6.8(9)
C(12)–C(11)–C(111)–N(112)	−26.7(10)
C(11)–C(111)–N(112)–Ti	30.4(7)
C(111)–N(112)–Ti–C(12)	−21.4(5)
N(112)–Ti–C(12)–C(11)	8.4(5)
C(15)–C(11)–C(111)–N(112)	164.1(8)
C(12)–C(1m)–C(2m)–C(25)	10.6(8)

[a]The suffix 'm' denotes the centroid of a Cp ring.

^{13}C, ^{1}H-HETCOR NMR measurements, has been previously observed in other ferrocene derivatives.[27]

The Mössbauer isomer shifts shown in Table 5 do not differ significantly from those of the lithiated starting material or of ferrocene itself [0.51(5) mm s^{-1} at 80 K, referenced against iron foil].[39] The lack of dependence of such shifts on the nature of the substituents on the rings is a common feature of ferrocenes.[39] However, the quadrupole splittings, which are mainly dependent on the asymmetry of the electron cloud around the iron nucleus, are much more sensitive to small changes in electronic distribution.

The data in Table 5 show lower values of q.s. (average 2.27 mm s^{-1}) for the Ti-complexes compared to the quadrupole splitting in ferrocene[39] [2.40(3) mm s^{-1}]. Such a reduction in q.s. is commonly associated with electron-withdrawing substituents on the ferrocenyl moieties,[26] and this seems to be the effect of the binding of the Ti^{IV} unit to the FcN ligands. Nevertheless, the magnitude of the measured change is so small that the data are difficult to rationalise.

If complex **3** contains two bidentate FcN moieties, this would generate a $16e^-$ complex. However, an alternative with monodentate FcN cannot be excluded and would constitute an additional example of stabilisation of low-coordination-number 3d metal species by bulky substituents. We can only exclude definitely a species with both monodentate and bidentate FcN, because this would be reflected by non-equivalencies in the NMR spectra.

Compound **4** may well contain both types of coordinated FcN. The introduction of the third (inherently asymmetric) FcN unit into the coordination sphere of the metal would eliminate a putative mirror plane that may be responsible for the equivalence of the FcN ligands in **3**. Therefore, **4** would be expected to show the presence of three non-equivalent FcN moieties, and this is actually the case. The ^{1}H and ^{13}C-{^{1}H} NMR spectra of [$CpTi(FcN)_3$] **4** clearly demonstrate the magnetic non-equivalence of the proton and carbon nuclei in different FcN ligands. As the solid state structure is still unknown, no attempt was made to assign specific resonances to a given FcN moiety. However, careful analysis of the spectra suggests that, in each set of three resonances associated with one specific kind of nucleus, two resonances seem to be close together and separated from the third. This effect is more noticeable in some resonances than in others. In the ^{1}H NMR spectrum, the "isolated" NMe_2 and $Fe(C_5H_5)$ peaks are shifted to the highest frequencies in each set, although the "distinct" NCH_2 pair of doublets is centred at the lowest frequency (Table 1). No clear pattern was observed for the "isolated" peaks in the ^{13}C NMR

Table 5 Mössbauer parameters[a] for Li(FcN) and complexes **1**–**6** (77 K, referenced against iron foil)

Compound	δ[b]/ mm s^{-1}	q.s.[c]/ mm s^{-1}	Γ[d]/ mm s^{-1}	Integrated area (%)
Li(FcN)	0.54(1)	2.33(1)	0.23(1)	100
[$Cp_2Ti(FcN)Cl$]	0.53(1)	2.28(1)	0.17(1)	100
[$CpTi(FcN)Cl_2$]	0.54(1)	2.29(1)	0.17(1)	100
[$CpTi(FcN)_2Cl$]	0.53(1)	2.24(1)	0.19(1)	100
[$CpTi(FcN)_3$]	0.52(1)	2.51(2)	0.16(1)	26(9)
	0.54(1)	2.28(1)	0.15(2)	41(15)
	0.53(1)	2.04(3)	0.17(1)	33(9)
[CpTi(FcN)(FcN′)]	0.54(1)	2.49(1)	0.16(1)	41(4)
	0.54(1)	2.22(1)	0.18(1)	59(4)
[$V(FcN)_2Cl$]	0.54(1)	2.37(1)	0.17(1)	100

[a] Numbers in parentheses correspond to the experimental error in the last significant figures(s). [b] Isomer shift. [c] Quadrupole splitting. [d] Half-width at half height.

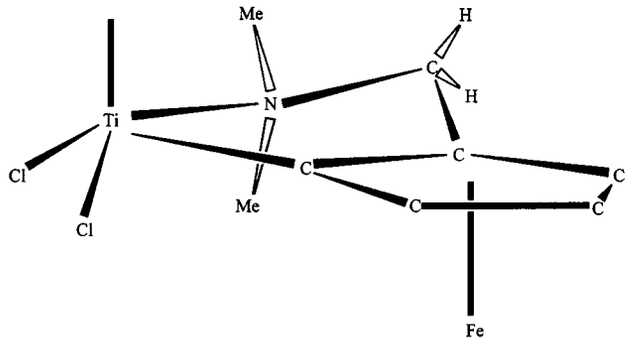

Fig. 4 Non-equivalence of methylene protons and methyl groups in complex **2**.

spectrum, but the separations themselves indicate that one of the FcN moieties is unique.

The Mössbauer data (Table 5) are consistent with the NMR spectroscopy. The detection of three different absorptions for complex **4** suggests that the iron nuclei experience three distinct electronic environments. This observation refers to the solid state at 77 K, conditions which differ clearly from the ones used in the NMR experiments. Even so, the two techniques are in apparent agreement. The quadrupole splittings fall into two groups, two significantly lower than in ferrocene and one significantly higher. The similar high q.s. value in the spectrum of complex **5**, which has been shown to contain two kinds ferrocenyl ligand (Fig. 4), supports the suggestion that one of the FcN ligands in **4** is different from the other two.

In order to detect possible dynamic behaviour, ^{1}H NMR spectra of complex **4** were recorded in C_6D_6 over 6 h in the temperature range 20–60 °C. Generally shifts of no more than *ca*. 0.1 ppm were observed. However, significant changes were detected for the NCH_2 and the disubstituted Cp proton resonances. The methylene resonances coupling constants, $^2J_{AB}$, are very similar (12.2 ± 0.4 Hz) for all the doublets detected between δ 2.6 and 3.7, but the peak separation $\Delta\nu_{AB}$ decreased with increase in temperature. The rate of decrease was *ca*. 1 Hz per °C for the pair of doublets centred at δ 3.21, but it was greater for the other methylene resonances, the highest rate being associated with the proton initially resonating at the lowest frequency. As a consequence, a gradual change in the pattern between δ 2.6 and 2.9 was observed so that two of the three protons resonated at the same frequency at 50 °C, without the loss of the AB pattern. These changes are reversible.

The resonances of the protons in the disubstituted Cp rings shifted significantly to higher frequencies as the temperature decreased, though the resonances of the protons in the other ferrocene ring did not move. In a previous report,[9] a similar temperature-dependent behaviour was related to rapid changes in the conformation of the CH_2 groups with respect to the other substituents in the C_3H_5 rings. Without more information, the data we have obtained for **4** cannot be reliably explained.

The only good crystalline material obtained when attempting to isolate complex **4** was actually, [CpTi(FcN)(FcN′)] **5**, where FcN′ = [(η^5-C_5H_5)Fe(η^5-$C_5H_3CH_2NMeCH_2$)] (Fig. 5). Complex **5** is probably derived from the electron-deficient Ti^{IV}–aryl complex **4**, and its formation is temperature-dependent. Hydrogen abstraction from a methyl group regenerates HFcN and the final product is further stabilised by the formation of a chelate ring which involves the Ti^{IV} ion (Fig. 6).

Confirmation that [$CpTi(FcN)_3$] **4** is the precursor of **5** was adduced by EI mass spectroscopy. The spectrum of a solid sample of **4** recorded with the probe at ambient temperature showed only ions derived from HFcN and its fragments. The probe was then carefully heated and when it reached 80 °C, molecular ions for both **4** (*m*/*z* 839) and **5** (*m*/*z* 596) were observed. As the probe temperature increased to 120 °C, the 839 ion lost intensity and the 596 ion increased. Once the probe

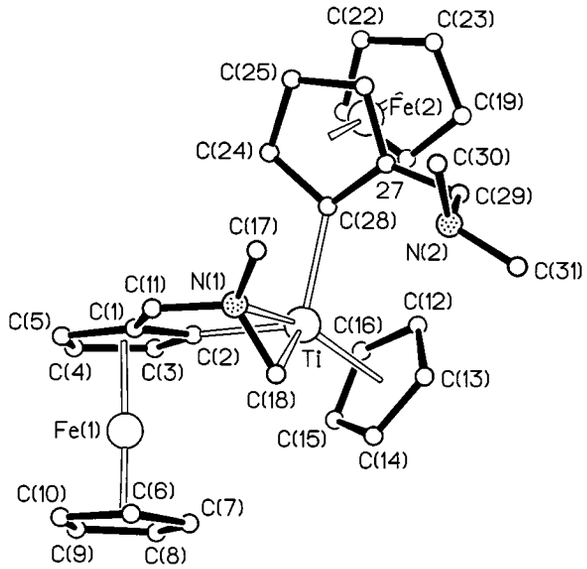

Fig. 5 Representation of the molecular structure of [$Ti(C_5H_5)$(FcN)(FcN′)], complex **5**, where FcN′$^{2-}$ = [Fe(η^5-C_5H_5){η^5-$C_5H_3CH_2N(CH_3)$-CH_2}]$^{2-}$.

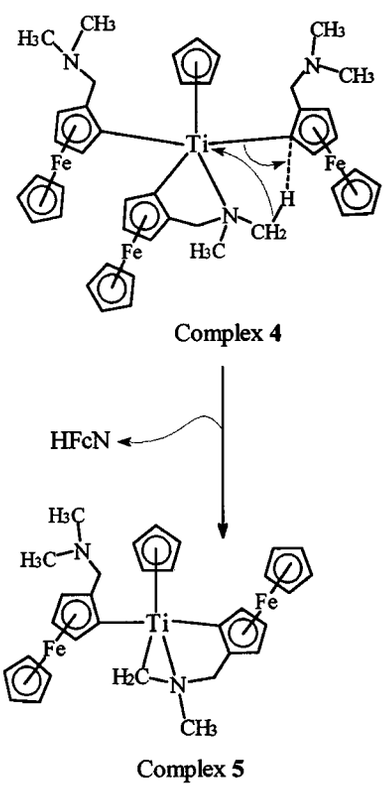

Fig. 6 The interconversion of complexes **4** and **5**.

temperature had risen to above 120 °C, only the 596 ion was observable. Above 120 °C the spectrum was that obtained essentially from pure **5**. The conversion of **4** to **5** was so facile that extreme care had to be taken to prevent it even under normal preparative conditions.

The ^{1}H NMR spectrum of **5** (Table 6) shows two singlets at δ 1.76 and 2.08, assigned to the methyl resonances in the monodentate FcN and in FcN′, respectively, and the three pairs of doublets generated by the groups of diastereotopic methylene protons (one doublet is hidden in the region where the protons of the disubstituted Cp rings resonate). The pair of doublets at the lowest frequencies is assigned to the highly shielded protons of the CH_2 group bound to Ti, as in the similar [{$CpFe(C_5H_4CH_2NMeCH_2)$}$Mn(CO)_4$].[29]

Brownish red crystals (small, thick plates) were obtained

Table 6 ^{1}H and ^{13}C NMR data for [CpTi(FcN)(FcN′)] **5** in C_6D_6 at room temperature

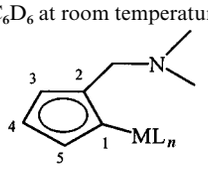

Proton or Carbon	Chemical shifts		
	^{1}H NMR	^{13}C-{^{1}H} NMR	^{13}C NMR (non-decoupled)
$N(CH_3)_2$	1.76 (s, 6H)	50.2	50.2 (q)
$N(CH_3)$	2.08 (s, 3H)	51.11	51.1 (q)
$N(CH_2)$	2.79 (d, 1H, J = 13.2)	65.4	65.4 (t)
	2.93 (d, 1H, J = 13.2)		
	3.76 (d, 1H, J = 14.2)[a]	64.4	64.4 (t)
H_2C–Ti	0.93 (d, 1H, J = 7.0)	89.7	89.7 (t)
	2.21 (d, 1H, J = 7.0)		
CpFe	3.91[b,c] (s)	69.4	69.4 (doublet of quintets)
	4.07 (s, 5H)	69.0	69.0 (doublet of quintets)
Positions 3, 4, 5	3.58 (m, 1H)	75.78	75.78 (d)
	4.00[b,d] (m)	64.70	64.70 (d)
	4.00[b,d] (m)	76.07	76.07 (d)
	3.91[b,c] (m)	60.70	60.70 (d)
	4.10 (t, 1H)	68.31	68.31 (d)
CpTi	6.75 (s, 5H)	112.9	112.9 (doublet of quintets)
Position 2	—	90.5, 93.4	90.5 (s), 93.4 (s)
Position 1	—	130.8, 131.8	130.8 (s), 131.8 (s)

[a] One doublet hidden in the H^3, H^4, H^5 region (δ 3.9–4.1); confirmed by ^{13}C, ^{1}H-HETCOR. [b] Block of 8H. [c] One multiplet hidden by the singlet at δ 3.91; confirmed by ^{13}C, ^{1}H-HETCOR. [d] Two signals superimposed at this position; confirmed by ^{13}C, ^{1}H-HETCOR.

from a saturated hexane solution of complex **5** kept at −20 °C for two weeks. Shortly after isolation, which was carried out by filtration at room temperature, the crystals seemed to start melting. They were then quickly cooled to −20 °C, and maintained at this temperature until being analysed by X-ray diffraction at 173(2) K. To ensure that the apparent "melting" of the sample was not due to decomposition, a second lot of crystals was later produced and submitted for X-ray structural analysis. They were kept in the mother-liquor at −20 °C until immediately before the analysis when a few crystals were quickly transferred to a drop of oil under the microscope. A suitable crystal was then selected, quickly mounted on a glass fibre and cooled to 173 K on the diffractometer. Although these crystals looked slightly different (thin plates with rounded edges) from the first batch, the cell parameters determined for both were the same.

Fig. 5 shows the molecular structure of complex **5** and Table 7 shows selected bond lengths and angles. The most remarkable feature of this structure is the titanium–carbon–nitrogen ring system. Similar three-membered metallacycles have been described for titanium(IV)[40] and vanadium(III)[41,42] compounds, as well as for other first-row transition metals,[43] such as in the closely related Mn complex, *N*-ferrocenylmethyl-*N*-methylaminomethylene(tetracarbonyl)manganese.[29]

The bonding of the N(1)–C(18) group and the geometry about the titanium suggest two possibilities: (i) the π-bonding of an iminium cation, $[FcCH_2N(Me)=CH_2]^+$ (Fc = 2-ferrocenyl) to the metal giving an overall pseudo-tetrahedral (or pyramidal) arrangement of the substituents; or (ii) the C,N-binding of a methyleneamino group, involving the nitrogen lone electron pair and a σ-bond between C(18) and Ti, generating a severely distorted square-pyramidal geometry.

Description (ii) would require a N(1)–C(18) bond distance close to 1.48 Å (single C–N bond in amines) and a C(11)–N(1)–C(17) angle of *ca*. 109.5°, characteristic of sp^3 hybridisation. The structural data seem more consistent with this. The angle C(11)–N(1)–C(17), 133.1(3)°, is similar to the analogous dimension in $[\{CpFe(C_5H_4CH_2NMeCH_2)\}Mn(CO)_4]$ (110.4°), which is assumed to possess a coordinated methyleneamino group.[44] The N(1)–C(18) bond length is 1.436(5) Å, closer to a normal C–N single bond length (1.48 Å), than to a C=N double-bond length, *ca*. 1.32 Å.

The Ti–C(2)–C(1)–C(11)–N(1) chelate ring in **5** is almost planar, with C(11) and N(1) only *ca*. 0.1 Å above the plane defined by C(1), C(2), and Ti. This plane is virtually coplanar with the fused C(1)–C(5) Cp ring. The dimensions (other than the torsion angles) in the chelate ring are similar to those determined for the analogous rings in complexes **2** and **6**. Any distortions in **5** can be ascribed to the strain caused by the fused Ti–N(1)–C(18) ring.

On the basis of the crystallographic data for **5** and related complexes,[41,43b,c,44] the most appropriate description of this molecular structure is as containing an N–CH_2 moiety in a methyleneamino group σ-bound to titanium and forming a three-membered metallacycle with it. The almost planar five-membered chelate ring is fused to this small ring with a dihedral angle 110.9(2)°. The overall geometry about the Ti^{IV} ion can be described as pseudo-tetrahedral, with C(18) and N(1) occupying a single coordination site.

The Cp rings in the "tridentate" ferrocenyl derivative are nearly eclipsed, with torsion angles typically close to the value of 2.2(4)° exhibited by C(1)–C(1m)–C(2m)–C(6). In the monodentate ligand on Fe(2), the deviation from the eclipsed conformation is very similar, for example with an angle C(20)–C(4m)–C(5m)–C(28) of −3.3(4)°. The angles between the normals to the least-squares planes calculated for these Cp rings are 3.7(3)° and 4.8(3)° in the "tridentate" and monodentate ferrocenyl moieties, respectively. This indicates that no particular strain has been placed on these groups by the formation of the fused ring system involving the titanium atom.

Complexes of vanadium

A number of different attempts to isolate vanadium(II) or vanadium(III) compounds containing dinitrogen and FcN has been made. None was entirely successful. However, the reaction between $[VCl_3(thf)_3]$ and Li(FcN) gave air-sensitive deep red paramagnetic products in low yield, with microanalytical data approximating to the values required for $[V(FcN)_2Cl]\cdot thf$.

The complex $[V(FcN)_2Cl]$ **6** was finally prepared in higher yield by a modification of the procedure described by Jacob and Palitzsch.[19] The product was first obtained as a red powder,

Table 7 Selected molecular dimensions in complex **5**. Bond lengths are in Ångstroms, angles in degrees. E.s.d.s are in parentheses

(a) About the metal atoms

Range of M–C lengths		Mean M–C	Distance to ring centroid[a]	
Fe(1)–C(1–5)	2.035(4)–2.094(4)	2.050(11)	Fe(1)–C(1m)	1.652(3)
Fe(1)–C(6–10)	2.035(4)–2.049(4)	2.043(2)	Fe(1)–C(2m)	1.653(4)
Fe(2)–C(19–23)	2.037(4)–2.041(4)	2.038(1)	Fe(2)–C(4m)	1.651(4)
Fe(2)–C(24–28)	2.026(4)–2.104(4)	2.048(14)	Fe(2)–C(5m)	1.650(4)
Ti–C(12–16)	2.359(4)–2.380(4)	2.373(4)	Ti–C(3m)	2.051(4)

Ti–N(1)	2.172(3)	Ti–C(2)	2.110(4)
Ti–C(18)	2.076(4)	Ti–C(28)	2.155(4)
C(1m)–Fe(1)–C(2m)	177.7(2)	C(4m)–Fe(2)–C(5m)	176.9(2)
N(1)–Ti–C(18)	39.4(1)	C(18)–Ti–C(28)	113.8(2)
N(1)–Ti–C(2)	80.7(1)	C(18)–Ti–C(3m)	114.0(1)
N(1)–Ti–C(28)	84.3(1)	C(2)–Ti–C(28)	107.5(1)
N(1)–Ti–C(3m)	153.2(1)	C(2)–Ti–C(3m)	112.1(2)
C(18)–Ti–C(2)	96.1(2)	C(28)–Ti–C(3m)	112.1(1)
Ti–C(2)–C(1m)	164.3(3)	Ti–C(28)–C(5m)	166.3(3)
C(1)–C(2)–Ti	112.1(3)	C(27)–C(28)–Ti	134.3(3)
C(3)–C(2)–Ti	142.9(3)	C(24)–C(28)–Ti	119.5(2)
C(11)–N(1)–Ti	114.8(2)	C(17)–N(1)–Ti	122.5(2)
C(18)–N(1)–Ti	66.7(2)	N(1)–C(18)–Ti	73.9(2)

(b) In the ferrocenyl side chains

C(1)–C(11)	1.491(5)	C(27)–C(29)	1.509(5)
C(11)–N(1)	1.479(5)	C(29)–N(2)	1.471(5)
N(1)–C(17)	1.462(5)	N(2)–C(30)	1.452(5)
N(1)–C(18)	1.436(5)	N(2)–C(31)	1.474(5)
C(2)–C(1)–C(11)	121.6(3)	C(28)–C(27)–C(29)	126.3(3)
C(5)–C(1)–C(11)	128.2(3)	C(26)–C(27)–C(29)	123.4(3)
C(1)–C(11)–N(1)	110.6(3)	C(27)–C(29)–N(2)	111.2(3)
C(11)–N(1)–C(17)	113.1(3)	C(29)–N(2)–C(30)	110.7(3)
C(11)–N(1)–C(18)	117.8(3)	C(29)–N(2)–C(31)	109.9(3)
C(17)–N(1)–C(18)	114.5(3)	C(30)–N(2)–C(31)	108.9(3)

(c) Torsion angles

Ti–C(2)–C(1)–C(11)	5.9(4)
C(2)–C(1)–C(11)–N(1)	−5.4(5)
C(1)–C(11)–N(1)–Ti	2.2(4)
C(11)–N(1)–Ti–C(2)	0.5(2)
N(1)–Ti–C(2)–C(1)	−3.3(3)
C(5)–C(1)–C(11)–N(1)	−178.8(4)
C(28)–C(27)–C(29)–N(2)	−82.9(5)
C(26)–C(27)–C(29)–N(2)	93.8(4)
C(1)–C(1m)–C(2m)–C(6)	2.2(4)
C(20)–C(4m)–C(5m)–C(28)	−3.3(4)

[a] The suffix 'm' denotes the centroids of the Cp rings: m = 1 for C(1–5), 2 for C(6–10), 3 for C(11–15), 4 for C(19–23), and 5 for C(24–28).

which was recrystallised from toluene–hexane to produce very thin reddish-brown plates suitable for X-ray structural analysis. The complex is very soluble in thf, soluble in aromatic hydrocarbons such as benzene and toluene, poorly soluble in diethyl ether and insoluble in hexane. It precipitates out at low temperature from toluene–diethyl ether or toluene–hexane mixtures as a shiny microcrystalline solid or very thin plates, often stacked together in multicrystalline arrangements. The crystals may also be temperature-sensitive.

The ^{1}H NMR spectrum resonances were slightly broadened, due to the paramagnetism of the sample, and shifted to higher frequencies when compared to those generated by HFcN (Table 1). The coupling constants of the protons in the methylene group ($^2J_{HH}$ = 13 Hz) are characteristic of geminal protons on sp^3 carbon atoms[26–28] and similar to those described above. The difference, $\Delta\nu$, between the chemical shifts of these two protons is very large (0.77 ppm) and the value of $\Delta\nu/J$ is 16, resulting in two clearly defined doublets.[27] However, the methyl groups in the $N(CH_3)_2$ units appear to be magnetically equivalent in the ^{1}H NMR spectra. This is unexpected and may be due to lack of resolution. The large shifts observed for the H(3)–H(5) protons in the disubstituted Cp ring (4.0–5.0 ppm) are consistent with the paramagnetic shift induced by the V^{III} ion.

This compares with the spectrum reported earlier[19] for this same complex, which was described as a singlet for the CH_2N protons (located exactly at the mid-point of the pair of doublets recorded in this work) and a small shift for the H(3)–H(5) protons (rather like the data reported for some diamagnetic Nb^V– and Ta^V–FcN complexes).[19] Similarly, the EI mass spectrum we obtained for **6** is consistent with the proposed formulation and the isotopic pattern obtained for the molecular ion (*m*/*z* 570) corresponds exactly to the theoretical isotopic pattern calculated for $C_{26}H_{32}ClFe_2N_2V$. Elsewhere[19] the spectrum has been reported to contain only ions derived from HFcN.

The Mössbauer spectrum of $[V(FcN)_2Cl]$ shows an isomer shift, like those of the titanium derivatives, close to the value obtained for Li(FcN). The small change in the quadrupole splitting (q.s.) indicates that, in this double-sandwich electronic environment, the Fe^{II} orbitals are not very sensitive to ring substituents. Similar results have been reported for stannyl derivatives of HFcN.[26]

Table 8 Selected molecular dimensions in complex **6**. Bond lengths are in Ångstroms, angles in degrees. E.s.d.s are in parentheses

(a) About the metal toms				
Range of M–C lengths		Mean M–C	Distance to ring centroid[a]	
Fe–C(1–5)	2.019(12)–2.086(12)	2.047(11)	Fe–C(1m)	1.65(1)
Fe–C(6–10)	2.022(14)–2.061(11)	2.043(8)	Fe–C(2m)	1.66(1)
V–N	2.233(10)	V–Cl	2.293(5)	
V–C(2)	2.087(13)			
C(1m)–Fe–C(2m)	176.5(5)			
N–V–N′	173.9(5)	N–V–Cl	93.1(2)	
N–V–C(2)	80.2(4)	C(2)–V–C(2′)	125.0(7)	
N–V–C(2′)	96.9(4)	C(2)–V–Cl	117.5(3)	
V–C(2)–C(1m)	161.8(10)	C(11)–N–V	114.8(2)	
C(1)–C(2)–V	109.8(9)	C(12)–N–V	116.2(7)	
C(3)–C(2)–V	145.9(8)	C(13)–N–V	109.6(7)	
(b) In the ferrocenyl side chains				
C(1)–C(11)	1.51(2)	N–C(12)	1.47(2)	
C(11)–N	1.47(2)	N–C(13)	1.49(2)	
C(2)–C(1)–C(11)	119.0(11)	C(11)–N–C(12)	110.2(10)	
C(5)–C(1)–C(11)	130.9(11)	C(11)–N–C(13)	108.2(9)	
C(1)–C(11)–N	108.6(9)	C(12)–N–C(13)	108.6(10)	
(c) Torsion angles				
V–C(2)–C(1)–C(11)	−1.2(13)			
C(2)–C(1)–C(11)–N	33.2(14)			
C(1)–C(11)–N–V	−44.3(10)			
C(11)–N–V–C(2)	35.8(7)			
N–V–C(2)–C(1)	−18.9(8)			
C(5)–C(1)–C(11)–N	−148.5(13)			
C(1)–C(1m)–C(2m)–C(6)	14.1(12)			

[a] The suffix 'm' denotes the centroids of the Cp rings: m = 1 for C(1–5), and 2 for C(6–10).

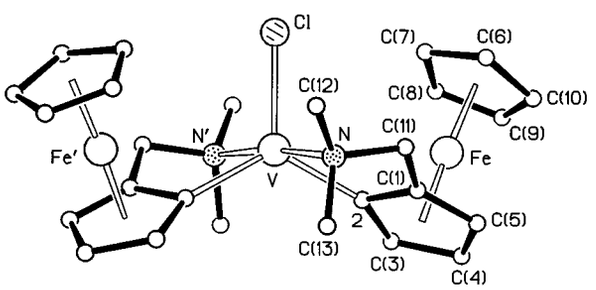

Fig. 7 ORTEP representation[60] of the molecular structure of complex **6**.

The solid state molecular structure of **6** is shown in Fig. 7 and selected bond lengths and angles are presented in Table 8. This is the first vanadium–FcN complex characterised by single-crystal X-ray diffraction. The geometry around the vanadium(III) ion in each molecule is trigonal bipyramidal, with the symmetry-related nitrogen atoms N and N′ of the chelating FcN occupying the apical positions. The equatorial plane contains, besides the V^{III} ion, both *ortho*-carbon atoms [C(2), C(2)′] and the chloride; angles in this plane are close to the ideal arrangement. A two-fold symmetry axis along the V–Cl bond relates the two FcN ligands.

The adoption of the trigonal-bipyramidal geometry instead of the alternative square-pyramidal arrangement seen in vanadium-(III) and -(IV) Schiff-base complexes[45,46] indicates that considerable steric constraints are generated in the solid state by the need to accommodate six five-membered rings around the vanadium atom. The same geometrical requirements may have determined the monomeric nature of the complex, as V^{II}– and V^{III}–halide complexes with less sterically-demanding ligands tend to form stable binuclear species.[47,48]

The dimensions inside the ferrocenyl units are very similar to those in ferrocene itself.[30] The cyclopentadienyl groups of each ferrocenyl unit deviate from the eclipsed conformation, with torsion angles typified by C(1)–C(1m)–C(2m)–C(6) at 14.1°. The angle of 5.7(8)° between the normals to the ring planes of each ferrocenyl unit is not exceptional, as interplanar angles larger than 7° have been found in constrained ferrocene molecules.[9]

The asymmetry of the five-memebered C(1)–C(11)–N(1)–V–C(2) rings fused to the ferrocenyl moieties confers planar chirality on the molecule.[24] The structure (Fig. 7) has an *R*,*R* configuration due to the arrangement of the ferrocene substituents, but the *S*,*S* isomer also occurs in the centrosymmetric unit cell. The configurations were assigned as described by Marquarding *et al*.[25]

The chelate ring is non-planar, having an envelope shape with the amine nitrogen atom *ca*. 0.74 Å out of the mean plane of the other four atoms, which is itself an extension of the plane of the Cp ring C(1)–C(5). The V^{III}–C(2)(Cp) distance is 2.09(1) Å, comparable to the V–C bond lengths in $[V^{III}(C_6H_4CH_2NMe_2\text{-}2)_2Cl(py)]$[49] [2.125(5) Å for the bond *trans* to Cl], $[V^{III}(mes)_3(thf)]$[41] (average 2.108 Å; mes = 2,4,6-$Me_3C_6H_2$) and in $[V^{III}\{\eta^2\text{-}C(mes)=NBu^t\}_3]$[41] (average 2.081 Å), although there are different geometries about the vanadium. Additionally, the V–C(2) bond in **6** is shorter, as expected, than the V–C bonds in the V^{II}-bridging N_2 complex $[\{V(C_6H_4CH_2NMe_2\text{-}2)_2(py)\}_2(\mu\text{-}N_2)]$[1] which also contains C and N as donor atoms bound to vanadium, and the V–C bonds in $[\{V^{II}(C_5H_4CH_3)_2\}_2\{\mu\text{-}[(C_5H_4)_2Fe]\}]$[50] (2.171 Å). The V–N(1) bond, at 2.23(1) Å, is shorter than the average V^{II}–N(tertiary amine) distance in $[V\{(C_6H_4CH_2NMe_2\text{-}2)_2(py)\}_2(\mu\text{-}N_2)]$[1] and in $[VCl_2(tmen)_2]$[51] (2.319 Å, in both cases). The V–Cl bond length [2.293(5) Å] is similar to the corresponding dimension in $[VCl_3(thf)_3]$[52] [2.297(2) Å for Cl *trans* to thf; 2.330(3) Å for Cl *trans* to Cl], but shorter than in $[VCl_2(tmen)_2]$[51] [2.487(1) Å], as expected.

Concluding remarks

Since the early reports on the reduction of N_2 by a number of reaction mixtures containing vanadium in low oxidation states

and, more recently, the unequivocal characterisation of vanadium(II)– and vanadium(III)–dinitrogen complexes, the search for efficient N_2-reducing chemical systems has included V-containing systems. The bulky, electron-rich $(FcN)^-$, with potential C,N-donor atoms and a still unexplored chemistry with early transition metals, seemed to provide an ideal chelating ligand to stabilise low-oxidation-state vanadium and increase the electronic density around the metal ion, in order to facilitate N_2 reduction. Unfortunately, systems containing vanadium(II) and FcN seemed to undergo too many side-reactions, and while combinations involving vanadium(III) were more productive in terms of complex preparation, they do not bind N_2. Nevertheless, complexes of titanium(IV) or vanadium(III) such as **2** and **6** should be reducible (by sodium amalgam, for example) and react with dinitrogen in the process. Such a way of producing a V^{II}–N_2 complex has been explored by Floriani and co-workers,[53] in the synthesis of [Na-{$(MeOCH_2CH_2)_2O$}$_2$][{$V(mes)_3$}$_2$(μ-N_2)Na].

We have shown that the *N*,*N*-dimethylaminomethyl derivative of ferrocene forms relatively stable complexes with vanadium(III) and titanium(IV). Complexes with vanadium(II) have proved to be extremely elusive, possibly due to side-reactions such as the cyclometallation we have identified with Ti^{IV} in complex **5**. Yields were not particularly high, and this can be related to high solubility and low stability of the products, especially towards moisture, and to temperatures above 20–30 °C. This work has provided examples of monodentate, bidentate, and even of a novel "tridentate" moiety, derived from FcN. The high basicity of the ferrocenylamine fragment favours decomposition of the products in the presence of proton sources (even other FcN units), with regeneration of neutral HFcN.

Experimental

All operations were carried out under an inert atmosphere in a dinitrogen-filled drybox (Faircrest Engineering, Croydon) or with use of standard Schlenk techniques. Solvents were dried by standard procedures[54] and distilled under N_2 prior to use. The commercial products *n*-butyllithium (1.6 M solution in hexane), sodium tetraphenylborate, titanium tetrachloride, titanocene dichloride, vanadium trichloride (Aldrich) and *N*,*N*-dimethylaminomethylferrocene (Aldrich or Lancaster) were used without further purification. *N*,*N*,*N*′,*N*′-Tetramethylethylane-1,2-diamine (tmen) and *p*-xylene were heated under reflux over molten sodium for *ca*. 1 h and then distilled under N_2. $[VCl_3(thf)_3]$[52,55] was prepared by heating VCl_3 overnight in refluxing tetrahydrofuran (thf), followed by hot filtration and crystallisation at room temperature. The yield was quantitative.

Microanalyses were by Ms. Nicola Walker (Department of Chemistry, University of Surrey), using a Leenan CE 440 CHN elemental analyser. Chlorine and titanium contents were determined by Butterworth Laboratories (Teddington, Middlesex), while vanadium and iron analyses were performed by Southern Science (Sussex Laboratory), by inductively coupled plasma optical emission spectroscopy.

NMR solvents, supplied by Goss Scientific Instruments, were dried over molecular sieves before use and kept under dinitrogen Schlenk tubes equipped with grease-free taps. NMR spectra were obtained in the appropriate deuteriated solvents using JEOL GSX-270 equipment. The operating frequencies for the observation of ^1H and ^{13}C were 270.2 and 67.9 MHz, respectively. Tetramethylsilane was used as reference.

^{13}C, ^1H-HETCOR NMR experiments were carried out by Dr. Shirley Fairhurst in the Nitrogen Fixation Laboratory, University of Sussex. IR data were recorded on a Perkin-Elmer 883 instrument, from Nujol mulls prepared under dinitrogen and spread on KBr plates. EI mass spectra were kindly recorded by Dr. A. Abdul Sada (University of Sussex) on a VG Autospec spectrometer (Fisons Instruments).

Mössbauer data were recorded at 77 K by Mrs. J. Elaine Barclay and Dr. David J. Evans (Nitrogen Fixation Laboratory) on an ES-Technology MS105 spectrometer with a 25 mCi ^{57}Co source in a rhodium matrix. Spectra were referenced against iron foil at 298 K. Samples were pure solids or mixtures with boron nitride (*ca*. 50% w/w), ground to fine powders and then transferred to the aluminium sample holders in the glove box. Programs used for spectra fitting and parameters calculation were ATMOSFIT 4, written by Dr. Ian Morrison (University of Essex) and MÖSSFIT, written by Dr. John G. Stamper (Nitrogen Fixation Laboratory).

Syntheses

Trichloro(cyclopentadienyl)titanium(III).[36] To a suspension of $[Cp_2TiCl_2]$ (9.9 g, 40 mmol) in *p*-xylene (70 cm^3), a large excess of $TiCl_4$ (18 cm^3, 31.1 g, 164.1 mmol) was carefully added by syringe. The mixture was left stirring under reflux for *ca*. 16 h and then cooled slowly to room temperature. Light brown crystals of $[CpTiCl_3]$ (15.9 g, 91% yield) were isolated by filtration after *ca*. 20 h, washed with toluene (3 × 10 cm^3) and dried under vacuum for 2 h. The product was later recrystallised by heating in *p*-xylene under reflux, followed by hot filtration and crystallisation at room temperature. Yield of the recrystallisation procedure, 65%.

Li(FcN).[56] *N*,*N*-Dimethylaminomethylferrocene (9.8 g, 40.3 mmol) was dissolved in diethyl ether (100 cm^3) and treated dropwise with a 1.6 M solution of *n*-butyllithium in hexanes (25 cm^3, 40 mmol) over 10 min. Stirring was continued for 16 h at room temperature and the resulting orange solid was then filtered off and washed with hexane (40 cm^3). A second crop of microcrystalline solid was isolated from the mother-liquor after allowing it to stand for 6 d at room temperature. Yield: 6.7 g, 67% (Found: C, 62.5; H, 7.00; N, 5.60. $C_{13}H_{16}FeLiN$ requires: C, 62.7; H, 6.50; N, 5.60%).

$[(C_5H_5)_2Ti\{(C_5H_3CH_2NMe_2)Fe(C_5H_5)\}Cl]$ 1. A stirred suspension of dichlorobis(cyclopentadienyl)titanium(IV) (1.9 g, 7.6 mmol) in diethyl ether (100 cm^3) was allowed to react with solid Li(FcN) (2.0 g, 8.0 mmol). After stirring for 2 h at room temperature (the red solution turned gradually deep green), the resulting mixture was filtered. The residue on the sinter (LiCl, 0.6 g) was washed with toluene (30 cm^3) and discarded. The filtrate (plus washings) was concentrated to *ca*. 25 cm^3 under vacuum and then layered with hexane (35 cm^3). Deep green crystals (2.1 g, 60%) separated upon standing at −20 °C for 3 d. Recrystallisation from a diluted diethyl ether–hexane (1:3) solution afforded deep green prisms suitable for X-ray analysis (Found: C, 61.0; H, 6.05; N, 3.20; Cl, 7.75. $C_{23}H_{26}ClFeNTi$ requires: C, 60.6; H, 5.75; N, 3.05; Cl, 7.80%). Mass spectrum [assignment, *m*/*z*, relative intensity (%)]: $[M]^+$ 455, 39; $[M - CH_3]^+$ 440, 3; $[M - Cl]^+$ 419, 2; $[M - Cp]^+$ 390, 3; $[M - NMe_2]^+$ 411, 3; $[(C_5H_4CH_2NMe_2FeCp]^+$ 243, 41; $[M - FcN]^+$ 213, 6.

$[(C_5H_5)Ti\{(C_5H_3CH_2NMe_2)Fe(C_5H_5)\}Cl_2]$ 2. A stirred suspension of trichloro(cyclopentadienyl)titanium (3.5 g, 16.0 mmol) in diethyl ether (150 cm^3) was allowed to react with Li(FcN) (4.0 g, 16.1 mmol) at room temperature. A change from yellow to deep blue-greenish was observed after 2–3 min. The reaction was carried out for 4 h and the mixture was then filtered to separate lithium chloride (light brown residue, 0.8 g), which was washed with toluene (75 cm^3) and discarded. The filtrate (plus washings) was kept at −20 °C for 20 h, giving a deep blue powder, that was filtered off, washed with cold hexane (50 cm^3) and dried under vacuum for 2 h (4.0 g, 58%). Small diamond-shaped crystals (thin plates), suitable for X-ray structural analysis, were isolated from a diluted diethyl ether–hexane solution kept at −20 °C for 6 d. The product is very soluble in

diethyl ether, even at low temperature, and changes to green and then to orange-yellow when exposed to air (Found: C, 50.6; H, 5.05; N, 3.25. $C_{18}H_{21}Cl_2FeNTi$ requires: C, 50.7; H, 5.00; N, 3.30%). Mass spectrum: $[M]^+$ 425, 45; $[M - CH_3]^+$ 409, 20; $[M - Cl]^+$ 390, 8; $[M - Cp]^+$ 359, 8; $[M - N(CH_3)_2]^+$ 381, 2; $[(C_5H_4CH_2NMe_2)FeCp]^+$ 243, 94; $[M - FcN]^+$ 183, 19.

$[(C_5H_5)Ti\{(C_5H_3CH_2NMe_2)Fe(C_5H_5)\}_2Cl]$ 3. To a yellow solution of $[CpTiCl_3]$ (1.7 g, 7.8 mmol) in diethyl ether (160 cm^3) two portions of the solid Li(FcN) (7.6 and 7.4 mmol) were dried sequentially. The additions were made as slowly as possible, under vigorous stirring, producing a gradual change of colour (yellow→light brown→deep green→deep blue) over 5 h. The reaction mixture was filtered, giving a small amount of a grey powder which was washed with toluene (5 cm^3) and discarded. The filtrate (plus washings) was then evaporated to dryness and the solid residue was suspended in Et_2O–hexane (1:2) (30 cm^3), cooled to −20 °C for 72 h, filtered and washed with cold (−20 °C) hexane (15 cm^3). After drying for 3 h under vacuum, 2.0 g of the product was isolated (41% yield). Thin deep blue needles were obtained by recrystallisation from saturated hexane solutions; they tend to become red after isolation (Found: C, 58.0; H, 5.95; N, 4.20. $C_{31}H_{37}ClFeN_2Ti$ requires: C: 58.8; H, 5.90; N, 4.45%). Mass spectrum: $[M]^+$ 632, 4; $[(C_5H_4CH_2NMe_2)FeCp]^+$ 243, 100; $[M - FcN]^+$ 389, 28.

$[(C_5H_5)Ti\{(C_5H_3CH_2NMe_2)Fe(C_5H_5)\}_3]$ 4. The reaction between $[CpTiCl_3]$ (0.5 g, 2.3 mmol) and Li(FcN) (1.8 g, 7.2 mmol) in diethyl ether (70 cm^3) produced a fine deep purple suspension after stirring for 15 min at 0 °C and then for 3 h at 10–20 °C. The solvent was then evaporated under vacuum to *ca.* 25 cm^3 and the mixture was filtered. The light brown residue was washed with cold (10–20 °C) toluene (4 × 5 cm^3) and discarded. The filtrate was taken to dryness, leaving a solid which was redissolved in diethyl ether (10 cm^3). Addition of hexane (10 cm^3) precipitated a deep purple powder which was filtered after 2 d at −20 °C, quickly washed with cold (−20 °C) hexane (2 × 10 cm^3) and dried under vacuum for 3 h. The temperature was kept as low as possible during and after filtration. A second batch of solid was obtained from the mother-liquor upon cooling to −20 °C for a further 7 d. Yield: 0.9 g (47%). Recrystallisation from a saturated hexane solution at −20 °C for 2–3 weeks afforded very small deep purple prisms.

The product is very soluble in low polarity solvents, even hexane, and this is an obstacle to isolation and purification. It changes to brownish red and then to orange when exposed to air for 15 min (Found: C, 60.7; H, 6.30; N, 4.60. $C_{44}H_{53}Fe_3N_3Ti$ requires: C, 62.9; H, 6.40; N, 5.00%). Mass spectrum: $[M]^+$ 839, 2; $[M - N(CH_3)_2]^+$ 795, 0.5; $[M - FcN]^+$ 596, 85.

$[(C_5H_5)Ti\{(C_5H_3CH_2NMe_2)Fe(C_5H_5)\}\{\{C_5H_3CH_2N(CH_2)Me\}Fe(C_5H_5)\}]$ 5. To a solution of $[CpTiCl_3]$ (0.9 g, 4.1 mmol) in diethyl ether (100 cm^3) at 30–35 °C was added Li(FcN) (3.0 g, 12.0 mmol). The reaction mixture was stirred for 18 h and a slow change to deep red was observed. The solution was evaporated under vacuum to *ca.* 50 cm^3 and the mixture was filtered, giving a solid residue (red + grey) which was extracted with toluene (2 × 5 cm^3) and hexane (4 × 10 cm^3). After extraction, the white-grey solid left on the sinter was discarded (apparently air-stable, 0.42 g). The filtrate (plus extracted material) was cooled to −20 °C for 3 d to give a brownish red microcrystalline solid which was filtered, washed with cold hexane (15 cm^3) and dried under vacuum. A second batch of product was isolated from the mother-liquor after concentration under vacuum and standing for 4 more d at −20 °C. Yield: 0.6 g (26%). Recrystallisation from a saturated hexane solution at −20 °C for *ca.* 2 weeks afforded thin reddish brown plates with rounded edges which were analysed by X-ray diffraction at −100 °C. This pure crystalline material melts (or suffers further chemical transformation with loss of HFcN) when isolated from the mother-liquor and kept at room temperature. The product is highly hygroscopic and changes to orange-yellow when exposed to air for *ca.* 1 h. It is also very soluble in solvents such as thf, diethyl ether, benzene, toluene and hexane (Found: C, 61.1; H, 6.10; N, 4.55. $C_{31}H_{36}Fe_2N_2Ti$ requires: C, 62.4; H, 6.10; N, 4.70%). Attempts to microanalyse the crystals used for the X-ray work were not successful, because their temperature-sensitivity made manipulation impossible.

$[V\{(2\text{-}C_5H_3CH_2NMe_2)Fe(C_5H_5)\}_2Cl]$ 6.[19] A red-orange solution of Li(FcN) (3.70 g, 14.9 mmol) in thf (60 cm^3) was added dropwise to a pink thf solution (60 cm^3) of $[VCl_3(thf)_3]$ (2.70 g, 7.2 mmol) kept at −78 °C. The colour changed quickly to reddish brown after the addition of the first drops of the Li salt solution. The mixture was allowed to warm slowly to room temperature (3 h) and left stirring for a further 18 h. The solvent was then taken to dryness under vacuum and replaced by Et_2O–toluene (1:1, 80 cm^3). The mixture was filtered, producing a magenta (red wine colour) filtrate **(A)** which was cooled to −20 °C, and a solid brownish red residue which was extracted with toluene (60 cm^3) and filtered. The filtrate **(B)** was layered with hexane (100 cm^3) and cooled to −20 °C. The solid residue left on the sinter (grey, 1.1 g) was discarded.

The Et_2O–toluene filtrate **A** produced a brownish red microcrystalline solid which was filtered, washed with cold hexane (3 × 5 cm^3) and quickly dried. A second batch of product was obtained from the mother-liquor **A** after concentration under vacuum and cooling for a further 10 d (−20 °C). Yield: 1.8 g, 44%. The toluene–hexane solution **B** gave reddish brown very thin plates which were analysed by X-ray diffraction at 173 K (Found: C, 53.5; H, 5.70; N, 4.60. $C_{26}H_{32}ClFe_2N_2V$ requires: C, 54.7; H, 5.65; N, 4.90%). Mass spectrum: $[M]^+$ 570, 44; $[M - N(CH_3)_2]^+$ 553, 17; $[(C_5H_4CH_2NMe_2)FeCp]^+$ 243, 100; $[M - FcN]^+$ 353, 21.

Preparation of samples for crystal structure analyses

Complex 1. An air-sensitive deep green prism (approximate dimensions 0.45 × 0.45 × 0.65 mm) was mounted on a glass fibre in the glove box and covered with epoxy resin. After preliminary photographic examination to check crystal quality, the crystal was transferred to an Enraf-Nonius CAD4-diffractometer.

Complex 2. Crystals were very dark blue diamond-shaped plates which are air-sensitive and rapidly oxidise to a clear pale brown. Several were sealed under dintrogen in glass capillaries and examined photographically and on the diffractometer. All were shown to comprise a number of closely aligned crystals. One, *ca.* 0.08 × 0.36 × 0.38 mm, showing one principal diffraction pattern with several weaker satellite patterns was selected for further analysis.

Complex 5. Crystals were small reddish brown air-sensitive prisms with rounded edges. They were stable below 0 °C but appeared to melt when warmed to *ca.* 20 °C. One crystal, *ca.* 0.40 × 0.40 × 0.20 mm, was selected from a batch stored at −20 °C and quickly mounted (covered with oil) on a glass fibre and then transferred to an Enraf-Nonius CAD4 diffractometer running at 173 K to prevent crystal decomposition.

Complex 6. Crystals were extremely thin, small, reddish brown air-sensitive plates. A small amount of crystalline material plus a few drops of mother-liquor were transferred to a drop of oil on a microscope slide. One of the crystals, *ca.* 0.4 × 0.3 × <0.01 mm, was quickly selected and mounted on a glass fibre, and then transferred to the diffractometer where it was cooled to 173 K.

Table 9 Crystallographic data and experimental details

Complex	**1**	**2**	**5**	**6**
Molecular formula	$C_{23}H_{26}ClFeNTi$	$C_{18}H_{21}Cl_2FeNTi$	$C_{31}H_{36}Fe_2N_2Ti$	$C_{26}H_{32}ClFe_2N_2V$
M	455.7	426.0	596.2	570.6
Crystal system	Orthorhombic	Monoclinic	Triclinic	Orthorhombic
Space group (no.)	$P22_12_1$ (equiv. to no. 18)	$P2_1/c$ (no. 14)	$P\bar{1}$ (no. 2)	*Pbcn* (no. 60)
a/Å	7.8564(9)	17.821(3)	9.598(6)	20.761(6)
b/Å	14.169(2)	7..6690(6)	11.697(7)	11.846(7)
c/Å	18.830(2)	13.938(2)	13.008(7)	9.63(2)
α/°			68.86(4)	
β/°		109.272(12)	73.85(5)	
γ/°			79.11(5)	
V/Å^3	2096.0(4)	1798.2(4)	1301.9(13)	2368(4)
Z	4	4	2	4
D_c/g cm^{-3}	1.44	1.573	1.52	1.60
F(000)	944	872	620	1176
μ(Mo-Kα)/cm^{-1}	12.1	15.4	14.2	17.3
T/K	293	293	173	295
λ/Å	0.71069	0.71069	0.71069	0.71069
θ_{max} for data collection/°	25	20	25	22
Crystal degradation (%)	2.7	4	0	0
Absorption: transmission factor range	0.93–1.00	0.62–0.88[a]	0.75–1.00	0.35–0.99
Total no. of unique reflections	2127	1674	4576	1443
No. of 'observed' reflections ($I > 2\sigma_I$)	1921	1349	3776	915
Structure determined by:	Direct methods	Patterson methods	Direct methods	Direct methods
Refinement	on F in SHELXN	on F in SHELXN	on F^2 in SHELXL	on F^2 in SHELXL
Final R, R_w, R_g[57]	0.041, 0.042, 0.047	0.056, 0.067, 0.084	—	—
Final R_1, wR_2[57]	—	—	0.059, 0.122	0.143, 0.233[b]
No. of reflections used	2127 (all data)	1674 (all data)	4576 (all data)	1443 (all data)
No. of parameters refined	272	247	325	146
Goodness-of-fit (on F^2)	—	—	1.05	1.05
w	$(\sigma_F^2 + 0.00036F^2)^{-1}$	$(\sigma_F^2 + 0.00595F^2)^{-1}$	c	c
Final difference map				
highest peaks/e Å^{-3} (location)	0.4 (close to a Cp ring)	0.45 (close to Ti atom)	0.63	1.7

[a]Absorption correction by analytical methods. [b] The high R-factors for this crystal result from weak diffraction from a very thin crystal. [c] As derived by SHELXL.[57]

X-Ray crystallographic analysis of $[(C_5H_5)_2Ti\{(C_5H_3CH_2NMe_2)Fe(C_5H_5)\}Cl]$ 1

On an Enraf-Nonius CAD4 diffractometer, accurate unit cell parameters and orientation matrix were refined from the settings of 25 reflections in the range $10 < \theta < 12°$, each reflection centred in four orientations. From the measurement of diffraction intensities to $\theta_{max} = 25°$, 2127 unique reflections were collected. The intensities of two representative reflections were monitored every 10000 seconds throughout the data collection, showing a decay of 2.7% overall.

During processing, data were corrected for Lorentz and polarisation effects, absorption (by semi-empirical ψ-scan methods) and elimination of negative intensities (by Bayesian statistical methods). The structure was solved by direct methods using the SHELXS program and refined by full-matrix least-squares procedures in SHELXN.[57]

From the refinement process it was apparent that the cyclopentadienyl groups of C(21)–C(25), in the ferrocenyl ligand, and C(31)–C(35), in the titanocene moiety, were disordered. In the case of the ferrocenyl group, a model incorporating two distinct orientations of the disordered Cp ring (50% of the molecules in each orientation) accounted well for the electron density in the region. For the disordered ring in the titanocene, two different orientations were also proposed with an occupancy factor of 0.7 initially assigned to the carbon atoms in the more populated ring orientation. On refinement of the site occupancy factors, values of 0.58(2) and 0.52(4) resulted for the more populated orientations of the ferrocenyl and titanocene disordered rings, respectively.

Except for those in the disordered groups mentioned above, all non-hydrogen atoms were refined with anisotropic thermal parameters. The atoms in the disordered Cp groups were refined isotropically. Hydrogen atoms were fixed in idealised positions, with methyl groups in staggered conformations. Their isotropic thermal parameters were refined freely.

The final cycle of refinement was based on all 2127 reflections, weighted $w = (\sigma_F^2 + 0.00036\ F^2)^{-1}$, and 272 parameters. The final R and R_w[57] factors were 0.041 and 0.042, respectively. In the final difference map, the residual electron density was *ca.* 0.4 e Å^{-3} for the largest peak, which was close to the C(21) and C(21x) ring groups.

Scattering factor curves for neutral atoms were taken from the literature.[58] Computer programs used in this analysis are listed in ref. 59 and were run on a DEC MicroVAX machine.

X-Ray crystallographic analyses of $[(C_5H_5)Ti\{(C_5H_3CH_2NMe_2)Fe(C_5H_5)\}Cl_2]$ 2, $[(C_5H_5)Ti\{(C_5H_3CH_2NMe_2)Fe(C_5H_5)\}\{[C_5H_3CH_2N(CH_2)Me]Fe(C_5H_5)\}]$ 5, and $[V\{2\text{-}(C_5H_3CH_2NMe_2)Fe(C_5H_5)\}_2Cl]$ 6

These followed similar procedures to those described above. Details are collected in Table 9.

CCDC reference number 182/175.[21]

Acknowledgements

We are grateful for support from the BBSRC, from CNPq (Brasilian Research Council) and from the British Council.

References

1 J. J. H. Edema, A. Meetsma and S. Gambarotta, *J. Am. Chem. Soc.*, 1989, **111**, 6878.
2 G. J. Leigh, R. Prieto-Alcón and J. R. Sanders, *J. Chem. Soc.*, *Chem. Commun.*, 1991, 921.
3 G. J. Leigh and J. R. Sanders, unpublished work; D. A. Hall, M. Jimenez-Tenorio, G. J. Leigh, R. Prieto-Alcón and J. R. Sanders, in *New Horizons in Nitrogen Fixation*, eds. R. Palacios, J. Mora and

W. E. Newton, Kluwer Academic Publishers, Dordrecht, 1993, p. 139.
4 J. H. Teuben and H. J. de Liefde Meijer, *J. Organomet. Chem.*, 1972, **46**, 313; J. H. Teuben, *J. Organomet. Chem.*, 1974, **69**, 241; J. D. Zeinstra, J. H. Teuben and F. Jellinek, *J. Organomet. Chem.*, 1979, **170**, 39.
5 J. H. Teuben, *J. Organomet. Chem.*, 1973, **57**, 59; J. H. Teuben, in *New Trends in the Chemistry of Nitrogen Fixation*, eds. J. Chatt, L. M. da Câmara Pina and R. L. Richards, Academic Press, London, 1980, p. 233.
6 D. W. Slocum and T. R. Engelmann, *J. Organomet. Chem.*, 1970, **24**, 753.
7 J. C. Gaunt and B. L. Shaw, *J. Organomet. Chem.*, 1975, **102**, 511.
8 P. R. R. Ranatunge-Bandarage, B. H. Robinson and J. Simpson, *Organometallics*, 1994, **13**, 500.
9 P. R. R. Ranatunge-Bandarage, N. W. Duffy, S. M. Johnston, B. H. Robinson and J. Simpson, *Organometallics*, 1994, **13**, 511.
10 L. G. Kuz'mina, Yu. T. Struchkov, D. A. Lemenovsky, I. F. Urazowsky, I. E. Nifantyev and E. G. Perevalova, *Koord. Khim.*, 1984, **9**, 1212.
11 L. G. Kuz'mina, Yu. T. Struchkov, D. A. Lemenovsky and I. F. Urazowsky, *J. Organomet. Chem.*, 1984, **277**, 147.
12 K.-H. Thiele, C. Krüger, R. Boese, G. Schmid, T. Bartik and G. Pályi, *Z. Anorg. Allg. Chem.*, 1990, **590**, 55; K.-H. Thiele, C. Krüger, T. Bartik and M. Dargatz, *J. Organomet. Chem.*, 1988, **352**, 115.
13 A. N. Nesmeyanov, N. N. Sedova, Yu. T. Struchkov, V. G. Andrianov, E. N. Stakheeva and V. A. Sazonova, *J. Organomet. Chem.*, 1978, **153**, 115.
14 A. N. Nesmeyanov, Yu. T. Struchkov, N. N. Sedova, V. G. Andrianov, Yu. V. Volgin and V. A. Sazonova, *J. Organomet. Chem.*, 1977, **137**, 217.
15 M. A. El-Sayed, A. Ali, G. Davies, S. Larsen and J. Zubieta, *Inorg. Chim. Acta*, 1992, **194**, 139.
16 K. Jacob, W. Kretschmer, K.-H. Thiele, I. Pavlik, A. Lycka and J. Holecek, *Z. Anorg. Allg. Chem.*, 1991, **606**, 133.
17 K.-H. Thiele and H. Baumann, *Z. Anorg. Allg. Chem.*, 1993, **619**, 1111.
18 K. Jacob, W. Kretschmer, K.-H. Thiele, I. Pavlik, A. Lycka and J. Holecek, *Z. Anorg. Allg. Chem.*, 1992, **613**, 88.
19 K. Jacob and W. Palitzsch, *Z. Anorg. Allg. Chem.*, 1994, **620**, 1489.
20 K. Jacob and C. Pietzsch, *Monatsh. Chem.*, 1997, **128**, 337.
21 P. B. Hitchcock, D. L. Hughes, G. J. Leigh, J. R. Sanders and J. S. de Souza, *Chem. Commun.*, 1996, 1985.
22 G. A. Razuvaev, G. A. Domrachev, V. V. Sharutin and O. N. Suvorova, *J. Organomet. Chem.*, 1977, **141**, 313.
23 R. S. Cahn, C. Ingold and V. Prelog, *Angew. Chem.*, *Int. Ed. Engl.*, 1966, **5**, 385.
24 V. I. Sokolov, L. L. Troitskaya and O. A. Reutov, *J. Organomet. Chem.*, 1979, **182**, 537.
25 D. Marquarding, H. Klusacek, G. Gokel, P. Hoffmann and I. Ugi, *J. Am. Chem. Soc.*, 1970, **92**, 5389.
26 J. Azizian, R. M. G. Roberts and J. Silver, *J. Organomet. Chem.*, 1986, **303**, 397.
27 R. V. Honeychuck, M. O. Okoroafor, L.-H. Shen and C. H. Brubaker, *Organometallics*, 1986, **5**, 482.
28 J. C. Randall, J. J. McLeskey, P. Smith and M. E. Hobbs, *J. Am. Chem. Soc.*, 1964, **86**, 3229.
29 S. S. Crawford and H. D. Kaesz, *Inorg. Chem.*, 1977, **16**, 3193.
30 A. Haaland and J. E. Nilsson, *Acta Chem. Scand.*, 1968, **22**, 2653.
31 A. Clearfield, D. K. Warner, C. H. Saldarriaga-Molina, R. Ropal and I. Bernal, *Can. J. Chem.*, 1975, **53**, 1622.
32 L. N. Zakharov, Yu. T. Struchkov, V. V. Sharutin and O. N. Suvorova, *Cryst. Struct. Commun.*, 1979, **8**, 439.
33 D. Cozak and M. Melnik, *Coord. Chem. Rev.*, 1986, **74**, 53.
34 J. W. Lauher and R. Hoffmann, *J. Am. Chem. Soc.*, 1976, **98**, 1729.
35 L. G. Kuz'mina, Yu. T. Struchkov, L. L. Troitskaya and V. I. Sokolov, *J. Struct. Chem.* (*Engl. Transl.*), 1985, **26**, 428.
36 R. D. Gorsich, *J. Am. Chem. Soc.*, 1958, **80**, 4744.
37 L. E. Manzer, R. C. Gearhart, L. J. Guggenberger and J. F. Whitney, *J. Chem. Soc.*, *Chem. Commun.*, 1976, 942.
38 W. F. J. van der Wal and H. R. van der Wal, *J. Organomet. Chem.*, 1978, **153**, 335.
39 R. V. Parish, *NMR*, *NQR*, *EPR and Mössbauer Spectroscopy*, Ellis Horwood, Chichester, 1990, p. 128; R. V. Parish, in *The Organic Chemistry of Iron*, eds. E. A. Koerner von Gustorf, F. W. Grevels and I. Fischler, Academic Press, New York, London, 1978, vol. 1, p. 175.
40 J. E. Hill, G. Balaich, P. E. Fanwich and I. P. Rothwell, *Organometallics*, 1993, **12**, 2911.
41 M. Vivanco, J. Ruiz, C. Floriani, A. Chiesi-Villa and C. Rizzoli, *Organometallics*, 1993, **12**, 1794.
42 M. Vivanco, J. Ruiz, C. Floriani, A. Chiesi-Villa and C. Rizzoli, *Organometallics*, 1993, **12**, 1802; J. Ruiz, M. Vivanco, C. Floriani, A. Chiesi-Villa and C. Rizzoli, *Organometallics*, 1993, **12**, 1811.
43 (*a*) E. W. Abel and R. J. Rowley, *J. Chem. Soc.*, *Dalton Trans.*, 1975, 1096; (*b*) M. Matsumoto, K. Nakatsu, K. Tani, A. Nakamura and S. Otsuka, *J. Am. Chem. Soc.*, 1974, **96**, 6777; (*c*) D. J. Sepelak, C. G. Pierpont, E. K. Barefield, J. T. Budz and C. A. Poffenberger, *J. Am. Chem. Soc.*, 1976, **98**, 6178.
44 S. S. Crawford, C. B. Knobler and H. D. Kaesz, *Inorg. Chem.*, 1977, **16**, 3201; S. S. Crawford and H. D. Kaesz, *Inorg. Chem.*, 1977, **16**, 3193.
45 L. Vilas Boas and J. C. Pessoa, in *Comprehensive Coordination Chemistry*, eds. G. Wilkinson, R. D. Gillard and J. A. McCleverty, Pergamon Press, Oxford, 1987, vol. 3, p. 453.
46 J. M. Rosset, C. Floriani, M. Mazzanti, A. Chiesi-Villa and C. Guastini, *Inorg. Chem.*, 1990, **29**, 3991; D. Bruins and D. L. Weaver, *Inorg. Chem.*, 1970, **9**, 130.
47 F. A. Cotton, S. A. Duraj, L. E. Manzer and W. J. Roth, *J. Am. Chem. Soc.*, 1985, **107**, 3850.
48 P. Sobota, J. Ejfler, S. Szafert, K. Szczegot and W. Sawka-Dobrowolska, *J. Chem. Soc.*, *Dalton Trans.*, 1993, 2353.
49 A. L. Spek, J. J. H. Edema and S. Gambarotta, *Acta Crystallogr.*, *Sect. C*, 1994, **50**, 1209.
50 F. H. Köhler, W. A. Geike, P. Hofmann, U. Schubert and P. Stauffert, *Chem. Ber.*, 1984, **117**, 904.
51 J. J. H. Edema, W. Stauthamer, F. van Bolhuis, S. Gambarotta, W. J. J. Smeets and A. L. Spek, *Inorg. Chem.*, 1990, **29**, 1302.
52 F. A. Cotton, S. A. Duraj, M. W. Extine, G. E. Lewis, W. J. Roth, C. D. Schmulbach and W. Schwotzer, *J. Chem. Soc.*, *Chem. Commun.*, 1983, 1377; F. A. Cotton, S. A. Duraj, G. L. Powell and W. J. Roth, *Inorg. Chim. Acta*, 1986, **113**, 81.
53 R. Ferguson, E. Solari, C. Floriani, A. Chiesi-Villa and C. Rizzoli, *Angew. Chem.*, *Int. Ed. Engl.*, 1993, **32**, 396.
54 P. D. Perrin and W. L. F. Armarego, *Purification of Laboratory Chemicals*, Pergamon Press, New York, 3rd edn., 1988.
55 L. E. Manzer, *Inorg. Synth.*, 1982, **21**, 138.
56 M. D. Rausch, G. A. Moser and C. F. Meade, *J. Organomet. Chem.*, 1973, **51**, 1.
57 G. M. Sheldrick, SHELX-76 Program for Crystal Structure Determination, University of Cambridge, 1976; SHELXN, an extended version of SHELX, 1977; G. M. Sheldrick, SHELXS, Program for Crystal Structure Determination, University of Göttingen, 1986; *Acta Crystallogr.*, *Sect. A*, 1990, **46**, 467; SHELXL-93–Program for Crystal Structure Refinement, University of Göttingen, 1993.
58 *International Tables for X-Ray Crystallography*, Kynoch Press, Birmingham, 1974, vol. 4, pp. 99, 149.
59 S. N. Anderson, R. L. Richards and D. L. Hughes, *J. Chem. Soc.*, *Dalton Trans.*, 1986, 245.
60 C. K. Johnson, ORTEP, Program for Diagrams, Report ORNL-3794, Oak Ridge Laboratory, TN, revised 1971.

Paper 8/08750D